ISSN 1062-8738, Bulletin of the Russian Academy of Sciences: Physics, 2026, Vol. 90, No. 2, pp. 254–259. © Pleiades Publishing, Ltd., 2026.

Pressure Induced Phase Separation in Lightly Doped $La_{0.95}Ca_{0.05}Mn_{0.98}Fe_{0.02}O_3$ Manganite

S. V. Zaitsev[a], *, V. D. Sedykh[a], A. V. Kuzmin[a], and K. P. Meletov[a]

[a] *Osipyan Institute of Solid-State Physics, Russian Academy of Sciences, Chernogolovka, Moscow oblast, 142432 Russia*

**e-mail: szaitsev@issp.ac.ru*

Received October 17, 2025; revised October 20, 2025; accepted October 27, 2025

Abstract—In polycrystalline $La_{0.95}Ca_{0.05}Mn_{0.98}Fe_{0.02}O_3$ manganite, high pressure leads to mesoscopic phase separation of the sample with the initial Jahn–Teller distortion of MnO_6 octahedra and the emergence of regions with undistorted octahedra above 4 GPa, with a complete rearrangement of the structure above ~12 GPa. Raman scattering and X-ray diffraction data indicate significant heterogeneity of lightly doped samples.

Keywords: high pressure, Raman scattering, manganite, structural phase separation

DOI: 10.1134/S1062873825715211

INTRODUCTION

Interest in perovskite-like lanthanum manganites was renewed after the discovery of the colossal magnetoresistance (CMR) phenomenon in them [1]. The physical properties of doped $La_{1-x}Me_xMnO_{3+\delta}$ manganites (where Me = Ca, Sr, Ba) are so diverse and often unusual that they are of great interest from both scientific and applied points of view [1–4]. For widespread use of the CMR effect, it is necessary to obtain stable single-phase materials of stoichiometric composition without excess oxygen ($\delta = 0$). Doped manganites of non-stoichiometric composition ($\delta > 0$) are also used as cathode materials for fuel energy, in which, due to the high diffusion of oxygen ions, the possibility of free entry and exit of oxygen is ensured [5, 6]. It should also be noted that the study of the structural, magnetic and electrical characteristics of manganites with various doping elements revealed a number of competing effects caused by the ions of such elements and oxygen [7].

Particular interest in doped lanthanum manganites is due to the tendency to form phase-separated states in them, which significantly affects their properties [4]. At $x \sim 0.1$, a transition from antiferromagnetic (AFM) order to ferromagnetic (FM) one is realized in these oxides [8]. Moreover, phase separation can play a significant role in the formation of unusual physical properties. Thus, detailed Mössbauer, X-ray, and magnetic studies of phase separation in calcium-doped lanthanum manganite $La_{1-x}Ca_xMn_{0.98}Fe_{0.02}O_3$ ($x = 0.05, 0.10, 0.20$) of stoichiometric composition in a wide temperature range, carried out in [9], showed that the structural phase separation is the coexistence of three orthorhombic phases *PnmaI*, *PnmaII* and *PnmaII**, characterized by different types of magnetic ordering at low temperatures. As the temperature decreases, the *PnmaI* phase transitions to the FM state, and the *PnmaII* and *PnmaII** phases transition to the AFM state. With an increase in the Ca content, the relative content of the FM phase and its Curie temperature increase. At low temperatures (~80 K), stoichiometric samples exhibit relaxation behavior, which may be due to the presence of small-sized magnetic clusters. In addition, it was shown [10] that in lanthanum manganite doped with a divalent element, with an increase in the content of the doping element, the number of Mn^{4+} ions increases, and the amount of interstitial oxygen decreases. Thus, the expansion of the concentration range towards a decrease in the doping element (Ca) in [9] made it possible to identify competing processes in samples of stoichiometric composition—the Jahn–Teller effect (orbital order) and the presence of Mn^{4+} ions (destruction of orbital order)—and to study the dynamics of changes in the structure and magnetic properties depending on the Ca content. However, a complete understanding of the physics underlying the microscopic properties of manganite has not yet been achieved, mainly due to the complexity arising from the competition between double exchange and superexchange, as well as the interaction between magnetic ordering, orbital ordering and the Jahn–Teller effect [11, 12]. Multiple competing ground states can be controlled or adjusted by

external influences such as electric and magnetic fields, temperature or pressure.

High pressure allows controlling the interaction between the crystal lattice and the electronic degrees of freedom in $RMnO_3$ and is therefore an effective method for studying the mutual influence of the lattice and electronic systems. Thus, it was shown [13] that the application of external hydrostatic pressure leads to a decrease in magnetoresistance and an increase in the Curie temperature of the compound in substituted $La_{1-x}Ca_xMnO_3$ manganites. In [14], the influence of hydrostatic pressure on the structural, vibrational, optical and electronic properties of $LaMnO_3$ was studied. The obtained data showed that the Jahn–Teller distortion of MnO_6 octahedra in $LaMnO_3$ continuously decreases with increasing pressure and appears to be completely suppressed at pressures above 18 GPa. However, the compound remains an insulator up to higher pressures of ~32 GPa, at which an insulator-metal transition occurs. The results of work [14] confirm the opinion that the Jahn–Teller effect is not of decisive importance for the stabilization of the ground state in $LaMnO_3$. These conclusions were revised and refined in [15], where the important role of pressure-formed domains with undistorted MnO_6 octahedra in the insulator-metal transition was demonstrated.

The purpose of this work was to study the structure and vibrational spectrum of lanthanum manganite of stoichiometric composition $La_{1-x}Ca_xMn_{0.98}Fe_{0.02}O_3$ with a low content ($x = 0.05$) of the doping divalent element (Ca) under pressure up to $P \sim 20$ GPa using Raman scattering (RS) and X-ray diffraction (XRD) methods.

EXPERIMENTAL

Polycrystalline samples were obtained by the sol-gel method from lanthanum and calcium nitrates, an aqueous solution of ^{57}Fe Mössbauer isotope nitrate and manganese acetate. Details of sample preparation, their composition and structure are described in [9]. To obtain a stoichiometric composition without excess oxygen ($\delta = 0$), $La_{1-x}Ca_xMn_{0.98}Fe_{0.02}O_{3+\delta}$ samples were annealed at $T = 650$°C in a vacuum (10^{-3} Torr). The samples are a conglomerate of melted particles ranging in size from fractions of a micrometer to tens of micrometers. Heat treatment does not significantly affect the change in particle size or appearance. According to iodometric titration data, the samples after vacuum annealing have a stoichiometric composition of $La_{1-x}Ca_xMn_{0.98}Fe_{0.02}O_3$. X-ray diffraction data indicate that in the studied samples at $x = 0.05$ the rhombic phase II* (sp. gr. *Pnma*) is formed, and at $x = 0.10$ and 0.20, a mixture of two rhombic phases I and II* (sp. gr. *Pnma*) appears [9]. Detailed Mössbauer studies have shown that at room temperature the structural phase separation of a sample with 5% calcium doping is the coexistence of three rhombic phases: FM phase I (9%), and AFM phases II (56%) and II* (35%) [9].

To characterize the powder samples at high pressure, X-ray diffraction patterns were obtained using MoK_α radiation with an Oxford Diffraction Gemini R diffractometer equipped with an Atlas S2 two-dimensional cooled CCD detector. The pressure was controlled using a specialized cell with Boehler-Almax Diamond Anvils, the pressure value was calibrated by the spectral position of the R1 luminescence line of the ruby crystal. The obtained diffraction patterns were processed and integrated using CrysAlis Pro software [Rigaku Oxford Diffraction, CrysAlisProSoftware System, Version 1.171.39.46 (Rigaku, United Kingdom, 2018)].

Raman spectra were measured in backscatter geometry using a setup consisting of an Acton SpectraPro-2500i spectrograph with a cooled Pixis2K CCD detector and an Olympus microscope. The measurements were carried out on individual crystallites with dimensions of ~20–50 μm. A continuous solid-state single-mode laser with a wavelength of $\lambda = 532$ nm was used to excite the Raman scattering. The laser beam was focused onto the sample using an Olympus SLMPLN objective with 50× magnification, a numerical aperture of 0.35, and a working distance of 18 mm. The laser emission line in the scattered beam was suppressed using an edge filter for $\lambda = 532$ nm with an absorbance OD = 6 and a bandwidth shift of ~100 cm^{-1}, the laser excitation intensity directly in front of the sample was ~1 mW. High-pressure measurements were carried out at room temperature in a Mao–Bell diamond anvil cell. A mixture of methyl and ethyl alcohols in a ratio of 4 : 1 was used as a pressure-transmitting medium, and pressure calibration was performed using the spectral position of the R1 luminescence line of ruby microcrystals. A total of three crystallites (samples no. 1, no. 2 and no. 3) were randomly selected from the array of polycrystalline powder $La_{1-x}Ca_xMn_{0.98}Fe_{0.02}O_3$ sample with $x = 0.05$ under pressure.

RESULTS AND DISCUSSION

Figure 1 shows the Raman spectra in the series of increasing (a) and decreasing (b) pressure in sample no. 1 at $T = 300$ K. For comparison, the spectrum before loading into the high-pressure chamber and after unloading ($P = 0$) is also shown. It can be seen that pressure leads to a blue shift and a significant rearrangement of the optical phonon mode $\nu_1 \sim 620$ cm^{-1} above $P_0 \sim 9$ GPa (Fig. 1a). Thus, with an increase in $P > P_0$, an additional mode $\nu_2 \sim 680$ cm^{-1} appears at

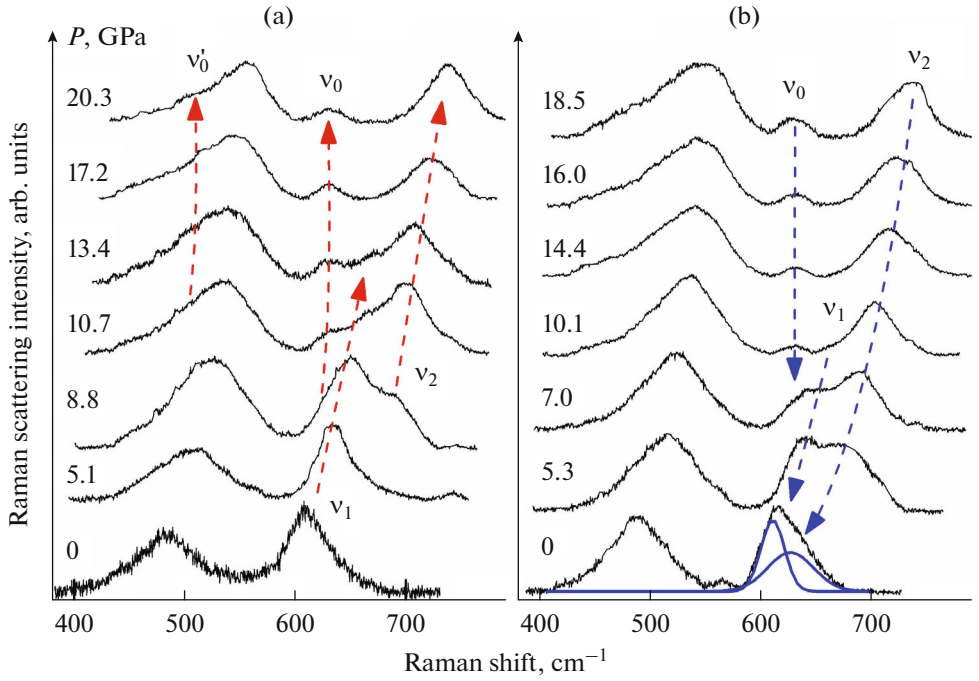

Fig. 1. Raman spectra (sample no. 1) of the $La_{0.95}Ca_{0.05}Mn_{0.98}Fe_{0.02}O_3$ sample under pressure in a series of (a) increasing and (b) decreasing pressure at $T = 300$ K. The colored (blue) lines show the Gaussian approximation of the high-energy band after pressure release.

higher energy, and its specific intensity increases with increasing pressure, while the initial mode ν_1 weakens and finally loses intensity above ~13.4 GPa (Fig. 1a).

The classification of phonon modes in $LaMnO_3$ has been studied in numerous papers and is well defined [16]. Thus, the modes below 200 cm^{-1} in $LaFeO_3$ are related to the lattice vibrations of heavy lanthanum, the modes in the range of 200–500 cm^{-1} are associated with various vibrations of lighter oxygen in the tilted octahedra of MnO_6 (~490 cm^{-1} is the apical bending of oxygen in the octahedra of MnO_6), and the most intense modes ~480 and ~610 cm^{-1} are attributed to the antisymmetric and in-phase stretching of Mn–O oxygen bonds in the plane [16]. Thus, the most unusual behavior with pressure is shown by the ν_1 mode, which corresponds to symmetrical stretching of the MnO_6 octahedra.

By analogy with undoped manganite $LaMnO_3$, we interpret the observed behavior as mesoscopic phase separation of samples with initial Jahn–Teller distortion of MnO_6 octahedra and the emergence of regions with undistorted octahedra at high pressure [14, 15]. Moreover, in contrast to undoped $LaMnO_3$, in lightly doped manganite of stoichiometric composition $La_{0.95}Ca_{0.05}Mn_{0.98}Fe_{0.02}O_3$ at $P > P_0$, a relatively weak (an order of magnitude weaker than the mode ~480 cm^{-1}) additional mode $\nu_0 \sim 630$–635 cm^{-1} arises, which almost does not shift with a further increase in pressure (Fig. 1a). It can be assumed that this mode is associated with apical bending vibrations of oxygen in MnO_6 octahedra, since when doped with gallium in $La_{1-x}Ga_xMnO_3$, such a mode almost did not change its energy (~500 cm^{-1}) in the full range of Ga concentrations, under so-called "chemical" pressure conditions [17]. However, since the energy of the apical mode (~500 cm^{-1}) in [17] differs significantly from that observed in the compound under study, the origin of this mode currently appears to be not entirely clear and requires further study. Note that simultaneously with the ν_0 mode, the apical vibration mode (~490 cm^{-1}) develops a similar low-energy shoulder $\nu_0' \sim 505$ cm^{-1}, which also weakly depends on pressure (Fig. 1a).

The reverse rearrangement of the spectra occurs when the pressure is removed, with the ν_2 mode exhibiting hysteresis and remaining in the spectrum at $\nu_2 \sim 630$ cm^{-1} even after the pressure is completely removed, as shown by the approximation of the wide high-energy band by Gaussians (spectrum at $P = 0$ in Fig. 1b). This metastable state of the sample, caused by areas with undistorted octahedra that arose under pressure, completely disappears within ~2 days after the pressure is removed.

Figure 2 shows the pressure dependences of the position of phonon modes in the Raman spectra for sample no. 1, obtained by approximating the spectral

bands with Gaussians. It shows the linear approximation of the dependences up to pressure P_0 and above with straight lines. Interestingly, the pressure shift coefficients $K_{1,2} = 4.1 \pm 0.2$ cm^{-1}/GPa for both modes (ν_1 and ν_2) coincide within the error limits, in contrast to the behavior of the modes in heavily doped $La_{0.75}Ca_{0.25}MnO_3$ manganite, in which $K_1 = 2.1 \pm 0.2$ cm^{-1}/GPa for the ν_1 mode, and $K_2 = 6.4$ cm^{-1}/GPa for ν_2 [18].

The application of pressure also leads to a sharp change in the baric dependence of the structural parameters at $P_1 \sim 4$–5 GPa (Fig. 3), which indicates a structural rearrangement of the rhombic phase in this lightly doped manganite. At the same time, the rearrangement occurs without changing the symmetry of the structure itself (rhombic phase II* with sp. gr. *Pnma*). In general, the X-ray diffraction data support the interpretation of the behavior observed under pressure as a mesoscopic phase separation of samples with an initial Jahn–Teller distortion of MnO_6 octahedra, accompanied by the emergence of submicrometer regions (smaller than the size of the laser spot) with undistorted octahedra, similar to undoped $LaMnO_3$ manganite [14, 15]. At the same time, the proposed explanation contains a discrepancy with the experiment: the pressure $P_1 \sim 4$ GPa, at which the structural rearrangement begins (Fig. 3), is significantly lower than the pressure $P_0 \sim 9$ GPa, at which the rearrangement of the optical phonon mode $\nu_1 \sim 620$ cm^{-1} begins (Fig. 2). Since X-ray structural analysis tests a macroscopically large amount of powder sample (hundreds and thousands of crystallites), an assumption arises about the significant heterogeneity of the studied polycrystalline sample with a low content of $x = 0.05$ of the doping divalent metal Ca, which was confirmed by further studies.

Figure 4 shows the Raman spectra of two other crystallites of this sample, samples no. 2 (a) and no. 3 (b), in series of increasing pressure. It can be seen that in sample no. 2, the rearrangement of the phonon mode $\nu_1 \sim 620$ cm^{-1} and the formation of a new mode $\nu_2 > 670$ cm^{-1} begins at a pressure of $P > 6$ GPa (Fig. 4a), whereas in sample no. 3, both phonon modes $\nu_1 \sim 610$ cm^{-1} and $\nu_2 \sim 670$ cm^{-1} are already present at the minimum pressure of $P = 0.4$ GPa in the sample chamber (Fig. 4b). Moreover, the ν_1 mode almost disappears (more than an order of magnitude weaker than the ν_2 mode ~700 cm^{-1}) at a pressure of $P = 8.5$ GPa. Thus, studies on various crystallites of the polycrystalline sample with a low content of $x = 0.05$ doping divalent Ca confirm the assumption of significant heterogeneity of such samples.

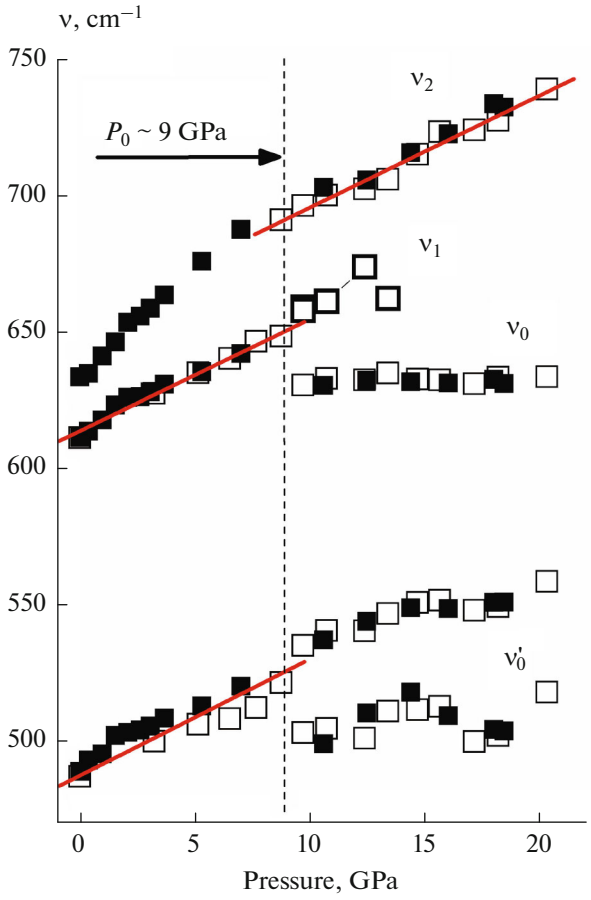

Fig. 2. Baric dependences of the position of phonon modes in the Raman spectra for $La_{0.95}Ca_{0.05}Mn_{0.98}Fe_{0.02}O_3$ sample no. 1 in the series of (a) increasing pressure (open symbols), and (b) decreasing pressure (closed symbols). $T = 300$ K. The straight red lines indicate the linear approximation of the dependences.

CONCLUSIONS

A polycrystalline sample of lightly doped lanthanum manganite $La_{0.95}Ca_{0.05}Mn_{0.98}Fe_{0.02}O_3$ was studied in detail using Raman spectroscopy and X-ray diffraction methods at high pressures up to 20 GPa and $T = 300$ K. Hydrostatic pressure in a wide range of $P \sim 4$–12 GPa leads to a rearrangement of the phonon mode ~610 cm^{-1}, corresponding to symmetrical stretching of MnO_6 octahedra and a sharp change in the baric dependence of the structural parameters at $P > 5$ GPa. This indicates a structural transition under pressure in the conditions of mesoscopic phase separation of samples with initial Jahn–Teller distortion of octahedra and the emergence of regions with undistorted octahedra under pressure. The pressure behavior is individual in each crystallite, which is due to the strong heterogeneity of polycrystalline samples of lightly doped lanthanum manganite.

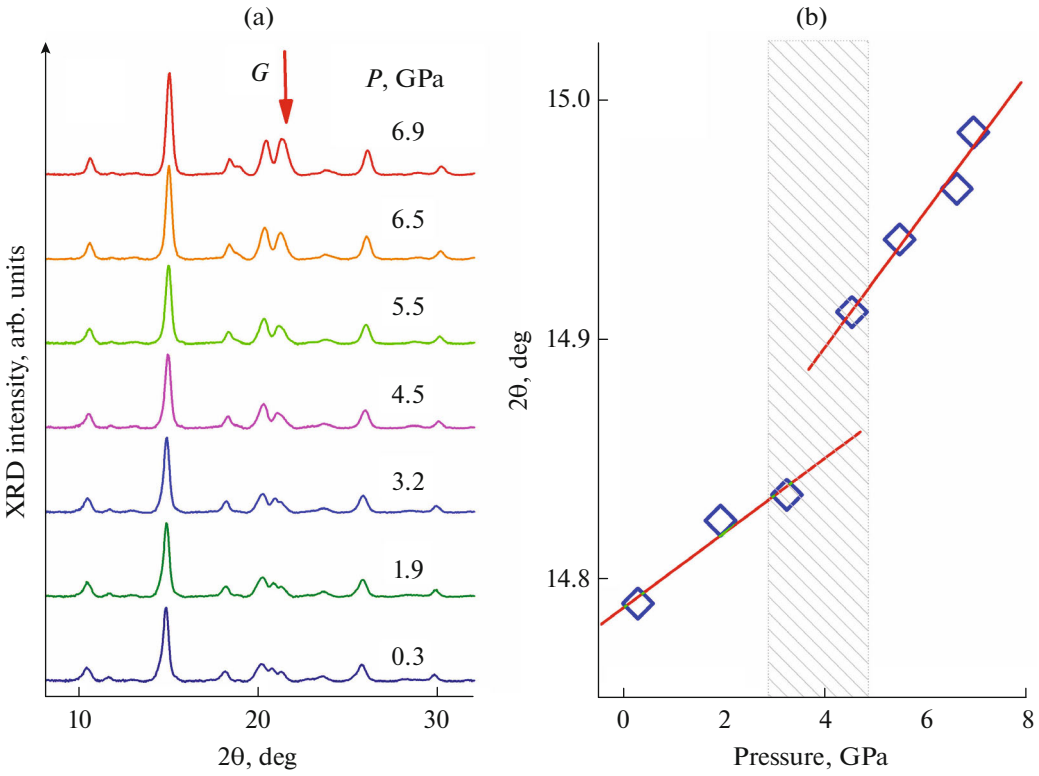

Fig. 3. (a) Diffraction patterns in a series of increasing pressure. The symbol G marks the peak corresponding to the steel pressure chamber material. (b) Baric dependences of the position of the X-ray peak ~15° in a polycrystalline orthorhombic $La_{0.95}Ca_{0.05}Mn_{0.98}Fe_{0.02}O_3$ sample (open symbols). Straight red lines show linear approximations of the dependences below P_0 ~ 4 GPa and above.

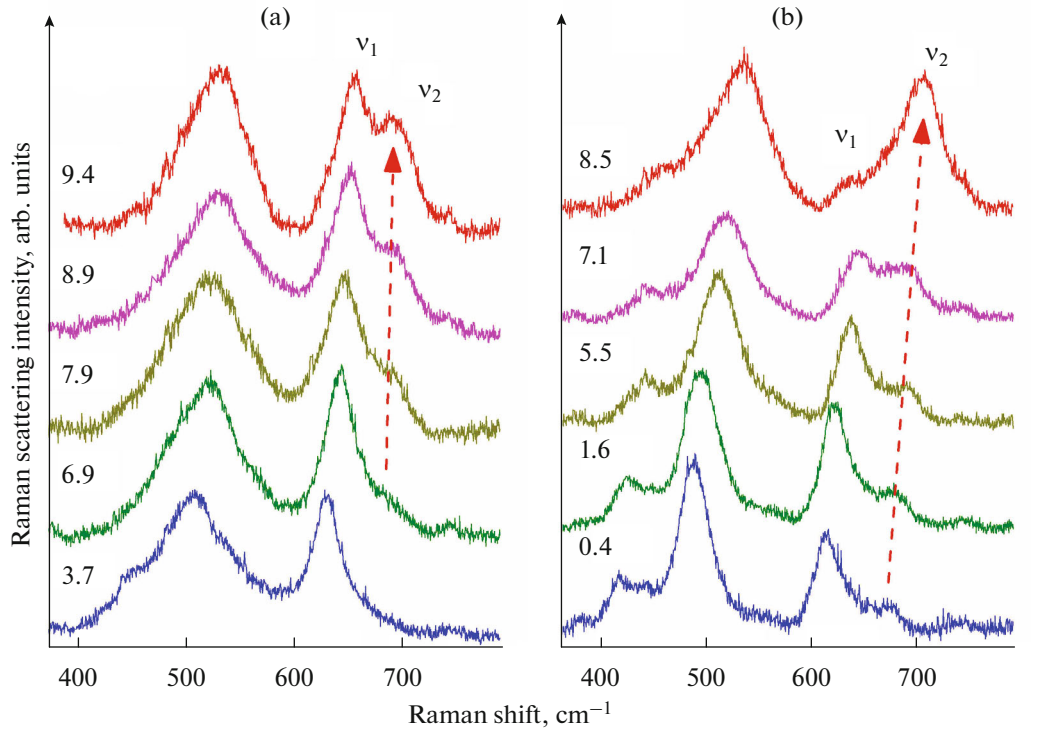

Fig. 4. Raman spectra: (a) sample no. 2 and (b) sample no. 3 of $La_{0.95}Ca_{0.05}Mn_{0.98}Fe_{0.02}O_3$ in a series of increasing pressure.

FUNDING

The work was carried out within the framework of the state assignment of the Osipyan Institute of Solid-State Physics of the Russian Academy of Sciences.

CONFLICT OF INTEREST

The authors of this work declare that they have no conflicts of interest.

REFERENCES

1. Jin, S., Tiefel, T.H., McCormack, M., et al., *Science*, 1994, vol. 264, p. 413.
2. Salamon, M.B. and Jaime, M., *Rev. Mod. Phys.*, 2001, vol. 73, p. 583. https://doi.org/10.1103/RevModPhys.73.583
3. Nagaev, E.L., *Phys.—Usp.*, 1996, vol. 39, no. 8, p. 781. https://doi.org/10.1070/PU1996v039n08ABEH000161
4. Loktev, V.M. and Pogorelov, Yu.G., *Low Temp. Phys.*, 2000, vol. 26, no. 3, p. 171. https://doi.org/10.1063/1.593868
5. Kharton, V.V., Viskup, A.P., Naumovich, E.N., and Tikhonovich, V.N., *Mater. Res. Bull.*, 1999, vol. 34, p. 1311.
6. Huang, K., Wang, J., and Goodenough, J.B., *J. Mater. Sci.*, 2001, vol. 36, p. 1093.
7. Badelin, A.G., Derzhavin, I.M., Karpasyuk, V.K., and Estemirova, S.Kh., *Bull. Russ. Acad. Sci.: Phys.*, 2023, vol. 87, no. 3, p. 343.
8. Moussa, F., Hennion, M., Biotteau, G., et al., *Phys. Rev. B*, 1999, vol. 60, p. 12299. https://doi.org/10.1103/PhysRevB.60.12299
9. Pchelina, D.I., Medvetskaya, I.Y., Chistyakova, N.I., et al., *J. Surf. Investig.*, 2019, vol. 13, p. 462.
10. Sedykh, V.D., Rusakov, V.S., Zverkova, I.I., et al., *Phys. Solid State*, 2011, vol. 53, no. 7, p. 1440. https://doi.org/10.1134/S1063783411070209
11. Millis, A.J., Littlewood, P.B., and Shraiman, B.I., *Phys. Rev. Lett.*, 1995, vol. 74, p. 5144. https://doi.org/10.1103/PhysRevLett.74.5144
12. Dagotto, E., Hotta, T., and Moreo, A., *Phys. Rep.*, 2001, vol. 344, p. 1. https://doi.org/10.1016/S0370-1573(00)00121-6
13. Laukhin, V., Fontcuberta, J., García-Muñoz, J.L., and Obradors, X., *Phys. Rev. B*, 1997, vol. 56, p. R10009. https://doi.org/10.1103/PhysRevB.56.R10009
14. Loa, I., Adler, P., Grzechnik, A., et al., *Phys. Rev. Lett.*, 2001, vol. 87, p. 125501. https://doi.org/10.1103/PhysRevLett.87.125501
15. Baldini, M., Struzhkin, V.V., Goncharov, A.F., et al., *Phys. Rev. Lett.*, 2011, vol. 106, p. 066402. https://doi.org/10.1103/PhysRevLett.106.066402
16. Iliev, M.N., Abrashev, M.V., Lee, H.-G., et al., *Phys. Rev. B*, 1998, vol. 57, p. 2872. https://doi.org/10.1103/PhysRevB.57.2872
17. Baldini, M., Di Castro, D., Cestelli-Guidi, M., et al., *Phys. Rev. B*, 2009, vol. 80, p. 045123. https://doi.org/10.1103/PhysRevB.80.045123
18. Congeduti, A., Postorino, P., Caramagno, E., et al., *Phys. Rev. Lett.*, 2001, vol. 86, p. 1251. https://doi.org/10.1103/PhysRevLett.86.1251

Translated by E. Domoroshchina